

 Open access • Posted Content • DOI:10.1101/2020.03.23.20040501

Climate affects global patterns of COVID-19 early outbreak dynamics — Source link

Gentile Francesco Ficetola, Gentile Francesco Ficetola, Diego Rubolini

Institutions: University of Savoy, University of Milan

Published on: 31 Mar 2020 - medRxiv (Cold Spring Harbor Laboratory Press)

Topics: Outbreak

Related papers:

- [High Temperature and High Humidity Reduce the Transmission of COVID-19](#)
- [Temperature, Humidity and Latitude Analysis to Predict Potential Spread and Seasonality for COVID-19](#)
- [Effects of temperature variation and humidity on the death of COVID-19 in Wuhan, China.](#)
- [The role of absolute humidity on transmission rates of the COVID-19 outbreak](#)
- [COVID-19 transmission in Mainland China is associated with temperature and humidity: A time-series analysis.](#)

Share this paper:    

View more about this paper here: <https://typeset.io/papers/climate-affects-global-patterns-of-covid-19-early-outbreak-4m57t7cge1>

Containment measures limit environmental effects on COVID-19 early outbreak dynamics

Gentile Francesco Ficetola^{1,2,*} and Diego Rubolini^{1*}

¹ *Dipartimento di Scienze e Politiche Ambientali, Università degli Studi di Milano, via Celoria
26, I-20133 Milano, Italy*

² *Université Grenoble Alpes, CNRS, Université Savoie Mont Blanc, LECA, Laboratoire
d'Ecologie Alpine, F-38000 Grenoble, France*

*Contributed equally to this work; order was decided with a coin toss

Correspondence: francesco.ficetola@gmail.com, diego.rubolini@unimi.it

1 **Abstract:** Environmental factors are well known to affect spatio-temporal patterns of infectious
2 disease outbreaks, but whether the recent rapid spread of COVID-19 across the globe is related
3 to local environmental conditions is highly debated. We assessed the impact of environmental
4 factors (temperature, humidity and air pollution) on the global patterns of COVID-19 early
5 outbreak dynamics during January-May 2020, controlling for several key socio-economic factors
6 and airport connections. We showed that during the earliest phase of the global outbreak
7 (January-March), COVID-19 growth rates were non-linearly related to climate, with fastest
8 spread in regions with a mean temperature of ca. 5°C, and in the most polluted regions.
9 However, environmental effects faded almost completely when considering later outbreaks, in
10 keeping with the progressive enforcement of containment actions. Accordingly, COVID-19
11 growth rates consistently decreased with stringent containment actions during both early and late
12 outbreaks. Our findings indicate that environmental drivers may have played a role in explaining
13 the early variation among regions in disease spread. With limited policy interventions, seasonal
14 patterns of disease spread might emerge, with temperate regions of both hemispheres being most
15 at risk of severe outbreaks during colder months. Nevertheless, containment measures play a
16 much stronger role and overwhelm impacts of environmental variation, highlighting the key role
17 for policy interventions in curbing COVID-19 diffusion within a given region. If the disease will
18 become seasonal in the next years, information on environmental drivers of COVID-19 can be
19 integrated with epidemiological models to inform forecasting of future outbreak risks and
20 improve management plans.

21 **Keywords:**

22 Temperature; absolute humidity; COVID-19, pathogen growth rate; global analysis; Climate;
23 Population size; Pollution; PM 2.5
24

25 **1. Introduction**

26

27 Host-pathogen interaction dynamics can be significantly affected by environmental conditions,
28 either directly, via e.g. improved pathogen transmission rates, or indirectly, by affecting host
29 susceptibility to pathogen attacks (Altizer et al., 2013). In the case of directly transmitted
30 diseases, such as human influenza and other viral diseases, multiple environmental parameters
31 including local temperatures and humidity impact on virus viability and transmission, with
32 significant consequences for the seasonal and geographic patterns of outbreaks (Shaman and
33 Kohn, 2009; Fuhrmann, 2010; Shaman et al., 2010; Lowen and Steel, 2014; Kampf et al., 2020).
34 The coronavirus SARS-CoV-2 is the aethiological agent of COVID-19, a pandemic zoonosis
35 causing severe pneumonia outbreaks at a global scale (World Health Organization, 2020).
36 During the initial months of 2020, this disease rapidly spread worldwide (Dong et al., 2020),
37 though the early dynamics of COVID-19 outbreaks appeared highly variable. Some countries
38 were experiencing slow growth and spread of COVID-19 cases, while others were suffering
39 widespread community transmission and fast, nearly exponential growth of infections (Dong et
40 al., 2020). Understanding the environmental drivers of early growth rates is pivotal to forecast
41 the potential severity of disease outbreaks and their interactions with containment measures
42 (Britton and Tomba, 2019; Baker et al., 2020; Jung et al., 2020). Given the importance of
43 environmental conditions on the transmission of many pathogens, we tested the hypothesis that
44 the severity of COVID-19 outbreaks across the globe was affected by spatial variation of key
45 environmental factors, and investigated the relative role of environmental conditions and of
46 containment measures adopted by governments on disease spread patterns.

47 A growing number of studies has been assessing the relationships between COVID-19
48 growth rate and multiple environmental features, such as temperature, humidity (e.g. Tamerius et
49 al., 2013; Islam et al., 2020a; Kampf et al., 2020; Runkle et al., 2020; Sajadi et al., 2020; Sobral
50 et al., 2020; Wu et al., 2020c), and air pollution (e.g. Bianconi et al., 2020; Rahman et al., 2020;
51 Wu et al., 2020b; Yao et al., 2020; Zhang et al., 2020), while accounting for major socio-
52 economic features of the affected regions (Coelho et al., 2020; Jaffe et al., 2020; Shammi et al.,
53 2020). However, results of these studies were sometimes controversial, casting doubts on the
54 possibility of correctly identifying environmental signals on COVID-19 spread dynamics
55 (Carlson et al., 2020a; Carlson et al., 2020b). Differences among studies can be caused by
56 multiple factors, including lack of standardized methodological framework, differences in spatial
57 extent and scale, and by complex interactions between human transmission, environmental
58 features and containment measures (Baker et al., 2020; Carlson et al., 2020b). Furthermore, both
59 environmental features and containment measures can show complex temporal trends in the
60 course of an outbreak. Studies assessing whether relationships between environment and
61 COVID-19 change are consistent across regions and time periods are pivotal to identify robust
62 and generalizable patterns.

63 We calculated the mean daily growth rate of confirmed COVID-19 cases during the
64 exponential phase of the epidemic growth curve for the 586 countries/regions (hereafter, regions)
65 (Supplement 1, Fig. S1) where at least 25 cases were reported before June, 2020. Variation at
66 these early epidemic growth rates represents the local progression of the disease and should best
67 reflect the impact of local environmental conditions on disease spread. However, environmental
68 effects on local disease spread could be blurred by containment actions, as in most regions local
69 authorities adopted unprecedented containment measures well in advance or immediately after

70 the detection of an outbreak to mitigate pathogen spread and community transmission (Hellewell
71 et al., 2020; Maier and Brockmann, 2020; Manenti et al., 2020; Thu et al., 2020).

72 In this study, we first assessed whether COVID-19 growth rate in different regions of the
73 world was affected by major environmental features (temperature, humidity, fine particulate
74 matter; see Methods), controlling for major socio-economic features of the affected regions.
75 Second, we tested whether the stringency of containment measures limited COVID-19 growth
76 rate at the onset of local outbreaks (Maier and Brockmann, 2020). Among the socio-economic
77 factors potentially affecting SARS-CoV-2 transmission dynamics during early outbreaks, we
78 considered human population size, population density, per capita government health expenditure
79 (hereafter, health expenditure) and age structure (see Methods). The importance of a given
80 region in the global air transportation network was expressed as its eigenvector centrality
81 (Coelho et al., 2020) (hereafter, region centrality; see Methods) while containment measures
82 were synthesized into a stringency index (Hale et al., 2020). Finally, to evaluate whether
83 relationships between environment and COVID-19 change were consistent across regions and
84 time periods, we considered regions experiencing outbreaks from January-March 2020 (when
85 outbreaks mostly started before the implementation of strict containment measures) to late May
86 2020, when lockdown-type containment actions were often adopted even before local outbreaks
87 started. We predicted that late outbreaks, starting under strict containment measures, should be
88 less severe than those starting under no or limited containment, and that environmental effects on
89 COVID-19 growth rate would fade through time, in pace with a progressive increase of the effect
90 of containment actions.

91

92 **2. Materials and methods**

93

94 *2.1 COVID-19 dataset*

95 We downloaded time series of confirmed COVID-19 cases (cumulative growth curves) from the
96 Johns Hopkins University Center For Systems Science and Engineering (JHU-CSSE) GitHub
97 repository (<https://github.com/CSSEGISandData/COVID-19/>) (Dong et al., 2020). JHU-CSSE
98 reports, for each day since January 22, 2020, confirmed COVID-19 cases at the country level or
99 at the level of significant geographical units belonging to the same country, which we broadly
100 defined here as ‘regions’ (e.g. US states, or China and Canada provinces; Supplement 1,
101 Supplementary methods). Data referring to outbreaks occurring on cruise ships were not
102 considered. The cumulative growth curves were carefully checked and obvious reporting errors
103 (a few occurrences of temporary decreases in the cumulative number of cases) were corrected.
104 Our dataset included confirmed COVID-19 cases up to June 15, 2020. From this dataset, we
105 selected data for all those regions in which local outbreaks were detected up to May 31, 2020
106 (see *Local outbreaks and COVID-19 cases growth rates*).

107 Overall, we considered data from 159 countries. We considered sub-national level data
108 for the all the countries of the world for which data were easily accessible from the original
109 sources listed in the JHU-CSSE website (for a total of 17 countries; Table S6). Our final dataset
110 included information on 586 regions (Supplement 1, Fig. S2 and Supplementary methods).

111

112 *2.2 Local outbreaks and COVID-19 cases growth rates*

113 To avoid the biases arising because of incomplete spread of the pathogen, our dataset included
114 only those regions experiencing a local COVID-19 outbreak. Therefore, our results are
115 unaffected by patterns occurring in regions where the pathogen showed a limited number of

116 records (e.g. because of distributional disequilibrium, limited connections with other affected
117 areas, or lack of reporting).

118 The onset of a local COVID-19 outbreak event was defined as the day when at least 25
119 confirmed cases were reported in a given region. Visual inspection of growth curves showed
120 that, in most cases, below this threshold the reporting of cases was irregular, or growth was
121 extremely slow for prolonged periods. This approach also allowed us to exclude the first cases,
122 often referring to individuals returning from foreign countries and not reflecting local
123 transmission of the pathogen. We then calculated the daily growth rate r of confirmed COVID-
124 19 cases for each region after reaching the 25 confirmed cases threshold following the approach
125 proposed by Hall et al. (2014). The method iteratively fits growth curves on successive intervals
126 of a minimum of 5 data points to identify the exponential phase of a cumulative growth curve,
127 and returns the lag phase, and the onset and end of the exponential growth phase. The lag phase,
128 characterized by very slow growth, is followed by the exponential phase (Supplement 1, Fig.
129 S1). Typically, cumulative growth curves of COVID-19 cases begin with exponential growth in
130 the early phases, which begins to decelerate within ca. 10 days of its beginning (e.g. Supplement
131 1, Fig. S3; see also Maier and Brockmann, 2020). This pattern is similar to what has been
132 documented for earlier phases of other major infectious disease outbreaks (Viboud et al., 2016).
133 We thus restricted the analyses to those regions for which at least 15 days of data after the
134 outbreak onset were available up to June 15, 2020.

135 Approaches assuming distributional equilibrium can be inappropriate to model the spread
136 of recently emerged infectious diseases (Carlson et al., 2020a). To avoid this issue, we used a
137 dynamic approach, whereby we modelled the dynamics of disease spread within populations
138 (Hall et al., 2014; Carlson et al., 2020a; Coelho et al., 2020). To this end, we computed the mean

139 daily growth rate of confirmed COVID-19 cases during the exponential phase as $r = [\ln(n$
140 $\text{cases}_{\text{day end exp. phase}}) - \ln(n \text{ cases}_{\text{day start exp. phase}})] / (\text{day end exp. phase} - \text{day start exp. phase})$. We
141 also computed the maximum daily growth rate r_{max} during the exponential phase according to
142 Hall et al. (2014). Lag and exponential phase duration, and r_{max} were computed through the R
143 package *growthrates* (Hall et al., 2014). Mean and maximum daily growth rates were strongly
144 positively correlated (Pearson's correlation coefficient, $r = 0.95$, $n = 586$ regions), indicating that
145 our growth rate estimates for a given region were highly consistent irrespective of the method
146 used for calculations. By modelling the exponential phase, this approach allowed to focus on
147 local transmission events occurring within the focal region. The average time interval between
148 the first case and the onset of the exponential phase was 19.5 days (SD = 11.1 days), thus cases
149 representing individuals returning from foreign countries likely have a negligible impact on our
150 growth rate estimates.

151

152 *2.3 Environmental variables*

153 We considered two climatic variables that are known to affect the spread of viral diseases: mean
154 air temperature and specific humidity (water vapor pressure), which is a measure of absolute
155 humidity. Previous studies showed that, for coronaviruses and influenza viruses, survival is
156 generally higher at low temperature and low values of absolute humidity (Lowen et al., 2007;
157 Shaman and Kohn, 2009; Tamerius et al., 2013; Lowen and Steel, 2014; Kampf et al., 2020; Yap
158 et al., 2020). For each region, we obtained the mean daily values for temperature ($^{\circ}\text{C}$) and
159 specific humidity (g/m^3) from the ERA5 hourly database (Supplement 1, Supplementary
160 methods).

161 The latency period of the infection, and the lag time between the onset of symptoms,
162 PCR tests and publication of confirmed cases can be highly variable across patients and across
163 areas of the world. For instance, Li et al. (2020a) suggested a mean incubation period of 4-7
164 days, but also reported cases with shorter incubation, or with incubation > 14 days. Therefore,
165 we measured the potential impact of temperature and humidity in two alternative time windows.
166 First, we considered a broad time period (30 days) occurring before the end of exponential phase.
167 For this 30-days time period, we computed mean climatic conditions (temperature and humidity
168 during 30 days; including the day of the end of the exponential phase and the preceding 29 days;
169 hereafter: 30-days period) (Supplement 1, Fig. S1). This 30-days period aims at covering all the
170 climatic conditions encountered by the broadest range of confirmed cases. Second, we used a
171 narrower time period, focusing on the most frequent time lags between infection and reporting.
172 Following Jüni et al. (2020), we computed mean climatic values assuming an exposure period for
173 infections starting 14 days before the onset of the follow-up period (in our case the start of the
174 exponential phase) and ending 14 days before the end of the follow-up period (in our case the
175 end of the exponential phase) (hereafter: $\Delta 14$ days period) (Supplement 1, Fig. S1).

176 Besides climate, it has been proposed that other environmental parameters may affect
177 variation of COVID-19 outbreak severity. Air pollution, especially fine atmospheric particulate,
178 may enhance the environmental persistence, transmission and effects of coronaviruses (Bianconi
179 et al., 2020; Zhang et al., 2020). We thus calculated the mean annual concentration of PM_{2.5} for
180 each region (Supplement 1, Supplementary methods).

181

182 *2.4 Socio-economic variables and airport connections*

183 Among socio-economic predictors, we considered mean human population density (Center for
184 International Earth Science Information Network, 2018) (hereafter, population density, expressed
185 in inhabitants/km²), total population size (Center for International Earth Science Information
186 Network, 2018), per capita government health expenditure (in US\$; average of 2015-2017
187 values) (Supplement 1, Supplementary methods). Elderly people are more susceptible to develop
188 severe COVID-19 symptoms (Wu et al., 2020a). We thus obtained for each country an estimate
189 of the proportion of the population aged 65 or older (population 65+).

190 Human mobility is well known to affect pathogen circulation and spatial dynamics
191 (Pybus et al., 2015), and such an effect has been highlighted also for early SARS-Cov-2 spread
192 (Gatto et al., 2020; Kraemer et al., 2020). We thus considered the potential relationships between
193 global airport connections and COVID-19 growth rate. Highly connected regions may
194 experience a higher 'propagule pressure' that increase disease diffusion among hosts, ultimately
195 influencing disease growth rates (Coelho et al., 2020). To investigate whether airport
196 connections affected early COVID-19 growth rates, we computed the eigenvector centrality
197 score for each region (region centrality). Highly connected regions have a higher region
198 centrality score (Bonacich, 1987) (Supplement 1, Supplementary methods).

199

200 *2.5 Stringency of containment measures*

201 For each region, we obtained an index of the overall stringency of COVID-19 containment
202 measures adopted by local authorities in the corresponding country at the onset of a local
203 outbreak (hereafter, stringency index). The stringency index was obtained by combining
204 information for each country from two separate data sources (Supplement 1, Supplementary
205 methods). This index simply record the number and strictness of government response measures,

206 hence a higher stringency score does not necessarily imply that a country's response is more
207 effective than that of other countries with lower scores (Hale et al., 2020). Nevertheless, the
208 stringency index may be helpful to illustrate the timeline of interventions and to assess whether
209 local governments' policy responses at outbreak onset had any impact on COVID-19 spread
210 within a given region.

211

212 *2.6 Statistical analyses*

213 We relied on linear mixed models (LMMs) to relate variation of COVID-19 growth rate across
214 regions to environmental and socio-economic/management predictors (temperature, humidity,
215 PM2.5, population density, population size, health expenditure, population 65+, region
216 centrality, stringency index). LMMs are an extension of linear models that allow to take into
217 account non-independence of data (Zuur et al., 2009). In our study case, multiple regions within
218 a given country were considered as non-independent as they share multiple features (e.g. health
219 policy, monitoring protocols, economic features other than those considered in the analyses).
220 Country identity was thus included as a random factor to account for non-independence of
221 growth rates from regions belonging to the same country. Non-linear relationships between
222 climatic factors and ecological variables are frequent (Legendre and Legendre, 2012), and have
223 also been suggested for relationships between SARS-CoV-2 occurrence and climate (e.g. Runkle
224 et al., 2020). As in exploratory plots we detected a clear non-linear relationship between r -values
225 and climate variables, we included in models both linear and quadratic terms. Humidity, PM2.5,
226 population density, population size, health expenditure and region centrality were \log_{10} -
227 transformed to reduce skewness and improve normality of residuals. Regression models can be
228 heavily affected by strong collinearity among predictors ($|r| \sim 0.70$ or above) (Dormann et al.,

229 2013). In our dataset, temperature and humidity showed a very strong positive correlation
230 (Supplement 1, Fig. S7 and Table S1). We thus fitted separate models for temperature and
231 humidity, and for different combinations of strongly correlated socio-economic predictors
232 (Supplement 1, Supplementary methods and Table S2).

233 To assess temporal variation in the importance of different predictors on COVID-19
234 growth rates, we fitted LMMs considering regions experiencing outbreaks in different periods.
235 Each LMM included data from regions experiencing outbreaks up to a given day. We started
236 from regions experiencing local outbreaks up to February 27, the first day when local outbreaks
237 occurred in at least 50 regions ($n = 51$ regions), and proceeded on a day-by-day basis until we
238 included all regions experiencing outbreaks up to May 31, 2020 ($n = 586$ regions; see the
239 cumulative curve in Supplement 1, Fig. S4). The partial R^2 statistic (variance explained by each
240 fixed effect, or semi-partial R^2) was taken as a measure of the importance of each fixed effect in
241 each of these models. Furthermore, we assessed temporal variation of standardized regression
242 coefficients for models fitted at different time points. Airport connections are expected to affect
243 the first phases of the epidemic events, and we therefore tested the effect of region centrality in a
244 model including data up to March 15, 2020 (Supplement 1, Supplementary results). To confirm
245 the time lag period used for the calculation of temperature and humidity (30-days period vs. $\Delta 14$
246 days period) did not affect our results, we repeated analyses twice, first using the 30-days period
247 data, and then using the $\Delta 14$ days period data. Climate variables calculated using the 30-days and
248 the $\Delta 14$ days periods showed almost perfect correlation across regions (temperature, $r = 0.99$;
249 humidity, $r = 0.99$; $n = 586$ regions).

250 LMMs were fitted using the `lmer` function of the *lme4* R package, while tests statistics
251 were calculated using the `lmerTest` package. Partial R^2 was computed using the *r2glmm* R

252 package. Finally, we used a generalized additive model (GAMs, fitted with the R *mgcv* package)
253 to evaluate the temporal trend of the stringency index at the outbreak date across regions
254 experiencing outbreaks in different periods. For this analysis we used GAMs as we expected a
255 complex temporal pattern and we did not have *a priori* expectations on the shape of relationship
256 between stringency index and time.

257

258 **3. Results**

259

260 COVID-19 growth rates showed high variability at the global scale (Supplement 1, Fig. S2). The
261 observed daily growth rate during the exponential phase was on average 0.22 (SD = 0.11, N =
262 586 regions), and ranged from < 0.01 (Argentina, Santiago del Estero and Canada, Prince
263 Edward Island) to 0.72 (Denmark). The exponential growth phase lasted on average 9.0 d (SD =
264 5.7) and was generally followed by a deceleration of growth, likely as a progressive effect of
265 containment actions and/or increasing awareness by local communities (Supplement 1, Fig. S3)
266 (Maier and Brockmann, 2020). The highest growth rates were observed in temperate regions of
267 the Northern Hemisphere, although relatively fast growth also occurred in some tropical
268 countries, notably Brazil, Indonesia and the Philippines (Supplement 1, Fig. S2). COVID-19
269 growth rates tended to decrease markedly from March to May (Fig. 1a). At the same time, the
270 stringency of containment measures strongly increased: since the end of March, most outbreaks
271 occurred in regions already under strict containment regimes (Fig. 1b).

272 Mixed models including environmental and socio-economic variables explained well
273 variation of COVID-19 growth rate across regions (Supplement 1, Fig. S4). Due to collinearity
274 among predictors (Supplement 1, Table S1), we explored different model formulations

275 (Supplement 1, Table S2 and Fig. S4). The model including temperature (either 30-days period
276 or $\Delta 14$ days period), its squared term and PM2.5 as environmental variables, and population
277 density, population size and health expenditure as socio-economic predictors showed the best fit
278 during the early outbreaks, and had similar explanatory power to alternative model formulations
279 when we considered later periods (Supplement 1, Fig. S4). We therefore rely on this model as
280 the main basis for subsequent inference.

281 Temperature was the strongest environmental predictor during early outbreaks,
282 explaining as much as 20% of the variance in COVID-19 growth rates (Fig. 2). Its effect began
283 to fade when we also included the outbreaks occurring in late March and became negligible from
284 mid-April onward (Fig. 2). PM2.5 exhibited a similar pattern, but its effect size was weaker
285 compared to temperature (Fig. 2). Higher PM2.5 levels were associated with fast growth rates
286 when considering early outbreaks only (Fig. 3). Population size and health expenditure were the
287 strongest socio-economic predictors of growth rates (Fig. 2), the highest growth rates being
288 consistently associated with larger population size and greater health expenditure during both
289 early and late outbreaks (Fig. 3). The stringency of containment measures at outbreak onset
290 consistently negatively predicted COVID-19 growth rates (Fig. 3), becoming the predictor with
291 the strongest effect on growth rates from mid-April onwards (Fig. 2). Results obtained using
292 either the 30-days or the $\Delta 14$ days period were nearly identical (Table S3a-b), even though the
293 model using the 30-days period showed slightly higher fit, and temperature effects during early
294 outbreaks were somewhat stronger when considering the 30-days period compared to the $\Delta 14$
295 days period (Fig. 2).

296 To illustrate the relationships between COVID-19 growth rate and environmental
297 variables, socio-economic variables, or stringency index, we produced partial regression plots

298 from models fitted on data up to three time points (March 15, to April 15 and May 15; Fig. 4,
299 Supplement 1, Fig. S5; see Supplement 1, Table S3a for model details). For outbreaks occurring
300 up to March 15, growth rates peaked in regions with mean temperature of ca. 5° C, decreasing in
301 both warmer and colder climates (Fig. 4a). Furthermore, highly polluted regions experienced a
302 faster disease spread (Fig. 4d). The effects of temperature and air pollution faded completely
303 when including later outbreaks (Fig. 4c-4f). Higher stringency of containment measures
304 consistently reduced growth rates at all three time points (Fig. 4g-i). Considering the effect of
305 airport connections during early outbreaks or considering alternative environmental and socio-
306 economic variables (absolute humidity, age structure) did not qualitatively alter these
307 conclusions (Supplement 1, Supplementary results and Tables S4-S5).

308

309 4. Discussion

310

311 The role of environmental drivers on COVID-19 spatial patterns and growth rate is controversial
312 (Araújo et al., 2020; Carlson et al., 2020a; Carlson et al., 2020b; National Academies of Sciences
313 Engineering and Medicine, 2020). Some authors suggested that this disease had a reduced impact
314 and spread in warm climates, and in areas with low pollution and experiencing intense UV
315 radiation (Merow and Urban, 2020; Rahman et al., 2020; Runkle et al., 2020; Sajadi et al., 2020;
316 Sobral et al., 2020; Wu et al., 2020b; Wu et al., 2020c; Zhang et al., 2020), while others reported
317 that socio-economic factors and airport connections have a much stronger impact than
318 environmental drivers (Coelho et al., 2020; Jaffe et al., 2020).

319 Our results considering the earliest COVID-19 data only (up to March, 2020) are in line
320 with initial evidence reporting less COVID-19 daily new cases and mortality in warm climates

321 (Wu et al., 2020c; Zhang et al., 2020), but exploring a broader time window explained the
322 inconsistency of results across studies. Many previous studies did not explicitly model non-linear
323 effects of climate, and were mostly restricted to the early phase of the global outbreak (Jüni et
324 al., 2020; Wu et al., 2020c). We instead included outbreaks occurring up to the end of May,
325 when COVID-19 reached an almost global spread (Supplement 1, Fig. S2), and adopted an
326 objective approach to identify the exponential phase of outbreaks (Hall et al., 2014). This
327 allowed focusing on early phases of the outbreaks (Maier and Brockmann, 2020), and
328 maximized the possibility of identifying environmental drivers before policy interventions
329 became effective (Merow and Urban, 2020). Finally, we explicitly modeled the spread dynamics
330 within regions (Carlson et al., 2020a; Coelho et al., 2020), thus avoiding the limitations of
331 approaches assuming distributional equilibrium between the pathogen and the environment
332 (Chipperfield et al., 2020).

333 Multiple non-exclusive processes could explain temperature effects on COVID-19 early
334 growth rate (Araújo et al., 2020; Sajadi et al., 2020). First, the persistence of SARS-Cov-2 and
335 other coronaviruses outside the hosts decreases at high temperature, medium-high humidity, and
336 under sunlight (Lowen et al., 2007; Chin et al., 2020; Kampf et al., 2020; Yap et al., 2020).
337 Second, host susceptibility can be higher in cold and dry environments, for instance because of a
338 slower mucociliary clearance, or a decreased host immune function under harsher conditions
339 (Fares, 2013; Tamerius et al., 2013; Lowen and Steel, 2014). Although SARS-CoV-2 is largely
340 transmitted indoor (Al Huraimel et al., 2020), climatic variation affects host immune response
341 and disease susceptibility (Tamerius et al., 2013). Moreover, it modulates human host behavior,
342 with cold temperatures leading to more time spent indoor and higher disease transmission risk
343 (Tucker and Gilliland, 2007; Fares, 2013; but see also Azuma et al., 2020 for a pattern where

344 contact among people increase in warm days). Thus, climate allows predictions of outbreaks of
345 respiratory illnesses (Shaman et al., 2010; Tamerius et al., 2013), acting both as direct and/or
346 indirect effect. The non-linear relationships between COVID-19 growth rate and temperature
347 detected for early outbreaks (Fig. 4a) might be explained by complex interplays between
348 weather-related changes in human social behavior, changes in host susceptibility to the virus, or
349 changes in virus survival and transmission patterns (Fares, 2013). Overall, with no or weak
350 containment measures, seasonal climatic variation may affect the spatial spread and the risk of
351 severe COVID-19 outbreaks (Merow and Urban, 2020; Wu et al., 2020c), as observed for other
352 viral diseases (Shaman et al., 2010; Tamerius et al., 2013; Lowen and Steel, 2014; Baker et al.,
353 2020), for which seasonal oscillations might lead to the worse outcomes during the colder
354 (autumn-winter) months. Nevertheless, containment measures are able to successfully limit
355 COVID-19 outbreaks in all climatic conditions (Maier and Brockmann, 2020), and climate alone
356 is unlikely to accurately predict transmission in future outbreaks.

357 The effect of air pollution on COVID-19 spread during early outbreaks was weaker than
358 the effect of local climate. In the early stages of the global outbreak, we observed more severe
359 outbreaks in regions with poor air quality, as gauged by their higher PM_{2.5} levels, in line with
360 studies suggesting that poor air quality may enhance local transmission and may increase
361 COVID-19 related mortality, possibly not independently of local meteorological conditions
362 (Azuma et al., 2020; Bianconi et al., 2020; Rahman et al., 2020; Wu et al., 2020b; Yao et al.,
363 2020; Zhang et al., 2020). Air pollution can influence COVID-19 spread through different
364 pathways. First, several studies have shown a worsening of respiratory symptoms from viral
365 diseases in populations exposed to poor air quality (Domingo and Rovira, 2020). For instance,
366 chronic exposure to PM 2.5 correlates with overexpression of the alveolar ACE-2 receptor,

367 leading to more severe COVID-19 infection and increasing the likelihood of poor outcomes
368 (Frontera et al., 2020; Wu et al., 2020b). Furthermore, the virus can remain viable in aerosols for
369 some hours, thus high pollution levels might increase its transmission (Frontera et al., 2020).
370 Nevertheless, more studies are required to clarify the actual impact of air pollution on COVID-
371 19 local spread patterns, as well as to identify the actual biological mechanisms (Wu et al.,
372 2020b).

373 However, the environmental effects on COVID-19 spread during the 2020 global
374 outbreak were not stable through time and disappeared when active containment actions were
375 enforced. Air quality effects became negligible when including outbreaks starting after mid-
376 March, while climate effects lasted a bit longer (until mid-April), but eventually disappeared as
377 well (Fig. 4a-b). From late March onward, most new outbreaks began under severe containment
378 actions (Fig. 1b). A weakening of environmental effects when considering late outbreaks is
379 consistent with the expectation that the enforcement of active containment policies limit the
380 spread potential of the disease and fade associations between climate and disease dynamics
381 (Baker et al., 2020; Maier and Brockmann, 2020).

382 Analyses of environmental effects on COVID-19 spread have been criticized because
383 SARS-CoV-2 shows a substantial rate of undocumented infections (Li et al., 2020b), and
384 because a high frequency of undocumented cases in some regions (e.g. in Africa) could affect
385 conclusions (Roche et al., 2018; Britton and Tomba, 2019). However, in the early phase of the
386 global outbreak, reported positives largely referred to tested individuals showing COVID-19
387 symptoms that require hospitalization. Therefore, even though our analyses cannot capture the
388 (unknown) dynamics of asymptomatic infections, they provide information on environmental
389 effects on the spread of symptomatic SARS-CoV-2 cases. Furthermore, our analyses took into

390 account health expenditure, which is strongly correlated to the daily testing rate across countries
391 (Supplement 1, Supplementary methods and Fig. S6). The high COVID-19 growth rate in
392 countries with higher health expenditure likely arose because of more efficient early reporting of
393 cases, thus considering health expenditure in the analyses should at least partly account for
394 differences in testing rate among regions. Finally, we focused on the few days of nearly
395 exponential growth, which generally lasted < 10 days. This limits the possibility that
396 'surveillance fatigue' (Romero-Alvarez et al., 2017) affected our results.

397 Our analyses provide compelling evidence for the effectiveness of policy interventions in
398 limiting disease spread within regions (Maier and Brockmann, 2020). Although our study was
399 not designed to explicitly test the effect of containment actions, it clearly showed that outbreaks
400 starting under strict containment actions were consistently less severe than those starting under
401 no or weak containment actions. This was already evident for the early (up to end of March)
402 outbreaks, and became the main factor explaining variation in COVID-19 growth rates among
403 countries when considering later outbreaks.

404 Containing COVID-19 outbreaks is undoubtedly one of the biggest societal challenges.
405 The huge variation of COVID-19 growth rates among regions with similar climate and air
406 quality levels highlights that diverse and complex social and demographic factors, as well as
407 stochasticity, may strongly contribute to the severity of local outbreaks, irrespective of
408 environmental effects. The potential socio-economic drivers of COVID-19 outbreak are many
409 (Coelho et al., 2020; Jaffe et al., 2020). Even if we did not manage to model the spatial spread of
410 the disease across regions, we integrated several variables reflecting potential socio-economic
411 drivers. The positive relationship with human population size might be explained by multiple,
412 non-exclusive processes including an easier control of early outbreaks in regions with small

413 populations, or the occurrence of more trade and people exchanges in the most populated
414 regions, resulting in multiple infection routes and faster spread (Coelho et al., 2020; Jaffe et al.,
415 2020). However, different socio-economic factors were strongly correlated. For instance, areas
416 with high health expenditure were also inhabited by more people older than 65 years
417 (Supplement 1, Table S1), and a linear combination of human population and health expenditure
418 predicts very well international trade of goods and services (Supplement 1, Supplementary
419 methods). Assessing the specific impact of these factors was beyond the aim of this study, but we
420 emphasize that environmental and containment actions effects were consistent irrespective of the
421 specific combination of socio-economic variables being considering, suggesting that
422 unaccounted socio-economic processes should not bias our findings.

423 In conclusion, our results suggest that local environmental conditions might have affected
424 COVID-19 spread in the early (but not the late) phase of the global outbreak, and that policy
425 interventions can effectively curb disease spread irrespective of environmental conditions (Islam
426 et al., 2020b; Maier and Brockmann, 2020; Thu et al., 2020). Stringent containment measures
427 thus remain pivotal to mitigate the impacts of SARS-Cov-2 infections (Hellewell et al., 2020;
428 Maier and Brockmann, 2020). Yet, information on environmental drivers of COVID-19 can
429 improve the ability of epidemiological models to forecast the risk and time course of future
430 outbreaks, and to suggest adequate preventive or containment actions (Baker et al., 2020).
431 Studies testing the association between environmental features and COVID-19 spread are a
432 rapidly expanding research area that has been attracting increasing attention (Franch-Pardo et al.,
433 2020; Wu et al., 2020b). The unprecedented nature of the pandemic has promoted a growing
434 number of ecological regression analyses, that have identified multiple complex relationships
435 between COVID-19 spread and transmission patterns and diverse environmental features,

436 providing a crucial stimulus to a rapidly evolving area of research (Franch-Pardo et al., 2020;
437 Wu et al., 2020b). The correlative nature of these analyses should call for cautionary
438 interpretations, as identifying the causal processes linking COVID-19 spread dynamics to
439 environmental features remain challenging, still associations detected in ecological analyses can
440 serve as a key starting point for future investigations during the future evolution of the
441 pandemics (Baker et al., 2020; Wu et al., 2020b).

442

443

444 **References**

445

446 Al Huraimel, K., Alhosani, M., Kunhabdulla, S., Stietiya, M.H., 2020. SARS-CoV-2 in the
447 environment: Modes of transmission, early detection and potential role of pollutions. *Sci. Total*
448 *Environ.* 744, 140946.

449 Altizer, S., Ostfeld, R.S., Johnson, P.T.J., Kutz, S., Harvell, C.D., 2013. Climate Change and
450 Infectious Diseases: From Evidence to a Predictive Framework. *Science* 341, 514-519.

451 Araújo, M.B., Mestre, F., Naimi, B., 2020. Ecological and epidemiological models are both
452 useful for SARS-CoV-2. *Nature Ecol. Evol.*

453 Azuma, K., Kagi, N., Kim, H., Hayashi, M., 2020. Impact of climate and ambient air pollution
454 on the epidemic growth during COVID-19 outbreak in Japan. *Environmental Research* 190,
455 110042.

456 Baker, R.E., Yang, W., Vecchi, G.A., Metcalf, C.J.E., Grenfell, B.T., 2020. Susceptible supply
457 limits the role of climate in the early SARS-CoV-2 pandemic. *Science* 369, 315-319.

458 Bianconi, V., Bronzo, P., Banach, M., Sahebkar, A., Mannarino, M.R., Pirro, M., 2020.
459 Particulate matter pollution and the COVID-19 outbreak: results from Italian regions and
460 provinces. *Arch. Med. Sci.* 16, 985-992.

461 Bonacich, P., 1987. Power and Centrality: A Family of Measures. *American Journal of*
462 *Sociology* 92, 1170-1182.

463 Britton, T., Tomba, G.S., 2019. Estimation in emerging epidemics: biases and remedies. *J. R.*
464 *Soc. Interface* 16, 10.

465 Carlson, C.J., Chipperfield, J.D., Benito, B.M., Telford, R.J., O'Hara, R.B., 2020a. Species
466 distribution models are inappropriate for COVID-19. *Nature Ecol. Evol.* 4, 770–771.

467 Carlson, C.J., Gomez, A.C.R., Bansal, S., Ryan, S.J., 2020b. Misconceptions about weather and
468 seasonality must not misguide COVID-19 response. *Nat. Commun.* 11, 4312.

469 Center for International Earth Science Information Network, C.C.U., 2018. Gridded Population
470 of the World, Version 4 (GPWv4): Population Density, Revision 11. NASA Socioeconomic Data
471 and Applications Center (SEDAC), Palisades, NY.

472 Chin, A.W.H., Chu, J.T.S., Perera, M.R.A., Hui, K.P.Y., Yen, H.-L., Chan, M.C.W., Peiris, M.,
473 Poon, L.L.M., 2020. Stability of SARS-CoV-2 in different environmental conditions. *The Lancet*
474 *Microbe* 1, e10.

475 Chipperfield, J.D., Benito, B.M., O'Hara, R., Telford, R.J., Carlson, C.J., 2020. On the
476 inadequacy of species distribution models for modelling the spread of SARS-CoV-2: response to
477 Araújo and Naimi. *EcoEvoRxiv*, <https://doi.org/10.32942/osf.io/mr32946pn>.

478 Coelho, M.T.P., Rodrigues, J.F.M., Medina, A.M., Scalco, P., Terribile, L.C., Vilela, B., Diniz,
479 J.A.F., Dobrovolski, R., 2020. Global expansion of COVID-19 pandemic is driven by population
480 size and airport connections. *Peerj* 8.

481 Domingo, J.L., Rovira, J., 2020. Effects of air pollutants on the transmission and severity of
482 respiratory viral infections. *Environmental Research* 187, 7.

483 Dong, E., Du, H., Gardner, L., 2020. An interactive web-based dashboard to track COVID-19 in
484 real time. *Lancet Infect. Dis.* 20, 533-534.

485 Dormann, C.F., et al., 2013. Collinearity: a review of methods to deal with it and a simulation
486 study evaluating their performance. *Ecography* 36, 27-46.

487 Fares, A., 2013. Factors influencing the seasonal patterns of infectious diseases. *Int J Prev Med*
488 4, 128-132.

489 Franch-Pardo, I., Napoletano, B.M., Rosete-Verges, F., Billa, L., 2020. Spatial analysis and GIS
490 in the study of COVID-19. A review. *Sci. Total Environ.* 739, 140033.

491 Frontera, A., Cianfanelli, L., Vlachos, K., Landoni, G., Cremona, G., 2020. Severe air pollution
492 links to higher mortality in COVID-19 patients: The 'double-hit'; hypothesis. *Journal of Infection*
493 81, 255-259.

494 Fuhrmann, C., 2010. The Effects of Weather and Climate on the Seasonality of Influenza: What
495 We Know and What We Need to Know. *Geography Compass* 4, 718-730.

496 Gatto, M., Bertuzzo, E., Mari, L., Miccoli, S., Carraro, L., Casagrandi, R., Rinaldo, A., 2020.
497 Spread and dynamics of the COVID-19 epidemic in Italy: Effects of emergency containment
498 measures. *Proceedings of the National Academy of Sciences* 117, 10484.

499 Hale, T., Webster, S., Petherick, A., Phillips, T., Kira, B., 2020. Oxford COVID-19 Government
500 Response Tracker. Blavatnik School of Government, University of Oxford,
501 www.bsg.ox.ac.uk/covidtracker, Oxford.

502 Hall, B.G., Acar, H., Nandipati, A., Barlow, M., 2014. Growth Rates Made Easy. *Mol. Biol.*
503 *Evol.* 31, 232-238.

504 Hellewell, J., et al., 2020. Feasibility of controlling COVID-19 outbreaks by isolation of cases
505 and contacts. *Lancet Glob. Health* 8, e488-e496.

506 Islam, A.R.M.T., Hasanuzzaman, M., Shammi, M., Salam, R., Bodrud-Doza, M., Rahman,
507 M.M., Mannan, M.A., Huq, S., 2020a. Are meteorological factors enhancing COVID-19
508 transmission in Bangladesh? Novel findings from a compound Poisson generalized linear
509 modeling approach. *Environmental Science and Pollution Research*.

510 Islam, N., Sharp, S.J., Chowell, G., Shabnam, S., Kawachi, I., Lacey, B., Massaro, J.M.,
511 D'Agostino, R.B., White, M., 2020b. Physical distancing interventions and incidence of
512 coronavirus disease 2019: natural experiment in 149 countries. *BMJ* 370, m2743.

513 Jaffe, R., Ortiz Vera, M.P., Jaffe, K., 2020. Globalized low-income countries may experience
514 higher COVID-19 mortality rates. *medRxiv*, 2020.2003.2031.20049122.

515 Jung, S.M., Akhmetzhanov, A.R., Hayashi, K., Linton, N.M., Yang, Y.C., Yuan, B.Y.,
516 Kobayashi, T., Kinoshita, R., Nishiura, H., 2020. Real-Time Estimation of the Risk of Death
517 from Novel Coronavirus (COVID-19) Infection: Inference Using Exported Cases. *J. Clin. Med.*
518 9, 10.

519 Jüni, P., Rothenbühler, M., Bobos, P., Thorpe, K.E., da Costa, B.R., Fisman, D.N., Slutsky, A.S.,
520 Gesink, D., 2020. Impact of climate and public health interventions on the COVID-19 pandemic:
521 a prospective cohort study. *Canadian Medical Association Journal* 192, E566.

522 Kampf, G., Todt, D., Pfaender, S., Steinmann, E., 2020. Persistence of coronaviruses on
523 inanimate surfaces and their inactivation with biocidal agents. *J. Hosp. Infect.* 104, 246-251.

524 Kraemer, M.U.G., et al., 2020. The effect of human mobility and control measures on the
525 COVID-19 epidemic in China. *Science* 368, 493.

526 Legendre, P., Legendre, L., 2012. *Numerical Ecology*. Elsevier, Amsterdam.

527 Li, Q., et al., 2020a. Early Transmission Dynamics in Wuhan, China, of Novel Coronavirus–
528 Infected Pneumonia. *N. Engl. J. Med.* 382, 1199-1207.

529 Li, R., Pei, S., Chen, B., Song, Y., Zhang, T., Yang, W., Shaman, J., 2020b. Substantial
530 undocumented infection facilitates the rapid dissemination of novel coronavirus (SARS-CoV2).
531 *Science* 368, 489.

532 Lowen, A.C., Mubareka, S., Steel, J., Palese, P., 2007. Influenza virus transmission is dependent
533 on relative humidity and temperature. *PLoS Pathog.* 3, 1470-1476.

534 Lowen, A.C., Steel, J., 2014. Roles of Humidity and Temperature in Shaping Influenza
535 Seasonality. *J. Virol.* 88, 7692-7695.

536 Maier, B.F., Brockmann, D., 2020. Effective containment explains subexponential growth in
537 recent confirmed COVID-19 cases in China. *Science* 368, 742-746.

538 Manenti, R., Mori, E., Di Canio, V., Mercurio, S., Picone, M., Caffi, M., Brambilla, M., Ficetola,
539 G.F., Rubolini, D., 2020. The good, the bad and the ugly of COVID-19 lockdown effects on
540 wildlife conservation: Insights from the first European locked down country. *Biol. Conserv.* 249,
541 108728.

542 Merow, C., Urban, M.C., 2020. Seasonality and uncertainty in global COVID-19 growth rates.
543 *Proc. Natl. Acad. Sci. USA* 117, 27456-27464.

544 National Academies of Sciences Engineering and Medicine, 2020. Rapid Expert Consultation on
545 SARS-CoV-2 Survival in Relation to Temperature and Humidity and Potential for Seasonality
546 for the COVID-19 Pandemic (April 7, 2020). The National Academies Press.
547 <https://doi.org/10.17226/25771>., Washington, DC.

548 Pybus, O.G., Tatem, A.J., Lemey, P., 2015. Virus evolution and transmission in an ever more
549 connected world. *Proc. R. Soc. B* 282, 20142878.

550 Rahman, M.S., Azad, M.A.K., Hasanuzzaman, M., Salam, R., Islam, A.R.M.T., Rahman, M.M.,
551 Hoque, M.M.M., 2020. How air quality and COVID-19 transmission change under different
552 lockdown scenarios? A case from Dhaka city, Bangladesh. *Sci. Total Environ.*, 143161.

553 Roche, B., Broutin, H., Simard, F., 2018. *Ecology and Evolution of Infectious Diseases: pathogen control and public health management in low-income countries*. Oxford university
554 press, Oxford.

556 Romero-Alvarez, D., Peterson, A.T., Escobar, L.E., 2017. Surveillance fatigue (fatigatio
557 vigilantiae) during epidemics. *Revista chilena de infectología* 34, 289-290.

558 Runkle, J.D., Sugg, M.M., Leeper, R.D., Rao, Y., Matthews, J.L., Rennie, J.J., 2020. Short-term
559 effects of specific humidity and temperature on COVID-19 morbidity in select US cities. *Sci.*
560 *Total Environ.* 740, 140093.

561 Sajadi, M.M., Habibzadeh, P., Vintzileos, A., Shokouhi, S., Miralles-Wilhelm, F., Amoroso, A.,
562 2020. Temperature, Humidity, and Latitude Analysis to Estimate Potential Spread and
563 Seasonality of Coronavirus Disease 2019 (COVID-19). *JAMA Network Open* 3, e2011834-
564 e2011834.

565 Shaman, J., Kohn, M., 2009. Absolute humidity modulates influenza survival, transmission, and
566 seasonality. *Proc. Natl. Acad. Sci. USA* 106, 3243.

567 Shaman, J., Pitzer, V.E., Viboud, C., Grenfell, B.T., Lipsitch, M., 2010. Absolute Humidity and
568 the Seasonal Onset of Influenza in the Continental United States. *PLoS Biol.* 8, 13.

569 Shammi, M., Bodrud-Doza, M., Towfiqul Islam, A.R.M., Rahman, M.M., 2020. COVID-19
570 pandemic, socioeconomic crisis and human stress in resource-limited settings: A case from
571 Bangladesh. *Heliyon* 6, e04063.

572 Sobral, M.F.F., Duarte, G.B., da Penha Sobral, A.I.G., Marinho, M.L.M., de Souza Melo, A.,
573 2020. Association between climate variables and global transmission of SARS-CoV-2. *Sci.*
574 *Total Environ.* 729, 138997.

575 Tamerius, J.D., Shaman, J., Alonso, W.J., Bloom-Feshbach, K., Uejio, C.K., Comrie, A.,
576 Viboud, C., 2013. Environmental Predictors of Seasonal Influenza Epidemics across Temperate
577 and Tropical Climates. *PLoS Pathog.* 9, 12.

578 Thu, T.P.B., Ngoc, P.N.H., Hai, N.M., Tuan, L.A., 2020. Effect of the social distancing measures
579 on the spread of COVID-19 in 10 highly infected countries. *Sci. Total Environ.* 742, 140430.

580 Tucker, P., Gilliland, J., 2007. The effect of season and weather on physical activity: A
581 systematic review. *Public Health* 121, 909-922.

582 Viboud, C., Simonsen, L., Chowell, G., 2016. A generalized-growth model to characterize the
583 early ascending phase of infectious disease outbreaks. *Epidemics* 15, 27-37.

584 World Health Organization, 2020. Coronavirus disease (COVID-2019) situation reports.
585 <https://www.who.int/emergencies/diseases/novel-coronavirus-2019/situation-reports/> [accessed 1
586 March 2020].

587 Wu, J.T., Leung, K., Bushman, M., Kishore, N., Niehus, R., de Salazar, P.M., Cowling, B.J.,
588 Lipsitch, M., Leung, G.M., 2020a. Estimating clinical severity of COVID-19 from the
589 transmission dynamics in Wuhan, China. *Nature Medicine*.

590 Wu, X., Nethery, R.C., Sabath, M.B., Braun, D., Dominici, F., 2020b. Air pollution and COVID-
591 19 mortality in the United States: Strengths and limitations of an ecological regression analysis.
592 *Science Advances* 6, eabd4049.

593 Wu, Y., Jing, W., Liu, J., Ma, Q., Yuan, J., Wang, Y., Du, M., Liu, M., 2020c. Effects of
594 temperature and humidity on the daily new cases and new deaths of COVID-19 in 166 countries.
595 Sci. Total Environ. 729, 139051.

596 Yao, Y., Pan, J., Wang, W., Liu, Z., Kan, H., Qiu, Y., Meng, X., Wang, W., 2020. Association of
597 particulate matter pollution and case fatality rate of COVID-19 in 49 Chinese cities. Sci. Total
598 Environ. 741, 140396.

599 Yap, T.F., Liu, Z., Shveda, R.A., Preston, D.J., 2020. A predictive model of the temperature-
600 dependent inactivation of coronaviruses. Applied Physics Letters 117.

601 Zhang, Z., Xue, T., Jin, X., 2020. Effects of meteorological conditions and air pollution on
602 COVID-19 transmission: Evidence from 219 Chinese cities. Sci. Total Environ. 741, 140244.

603 Zuur, A.F., Ieno, E.N., Walker, N.J., Saveliev, A.A., Smith, G.M., 2009. Mixed effects models
604 and extensions in ecology with R. Springer, New York.

605

606 **Acknowledgments**

607 We thank the colleagues of the DISPARati group, especially G. Scari, for insightful and
608 stimulating discussions. We also thank M. Venegoni, G. Venegoni, V. Longoni, J. G. Cecere and
609 L. Serra for commenting on previous draft of our manuscript, and three anonymous reviewers for
610 insightful suggestions.

611

612 **Author contributions**

613 The authors jointly a conceived the work, analyzed data and wrote the manuscript.

614

615 **Competing interests**

616 None

617

618 **Data and materials availability**

619 All relevant data have been submitted as supplementary files.

620

621

622 **Fig. 1.** COVID-19 growth rate (a) and stringency of containment measures (b) in regions
623 experiencing COVID-19 outbreaks in different periods. The bold lines represent the fit of a
624 generalized additive model, the shaded area its 95% confidence band. The figures report data for
625 regions where outbreaks occurred between February 27 and May 31, 2020, as before that date
626 data were sparse (< 50 regions experienced outbreaks between January 22 and February 26).

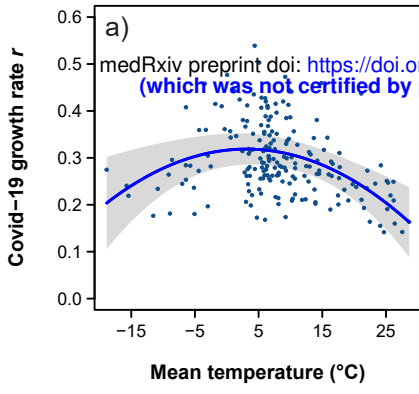
627
628 **Fig. 2.** Temporal variation of the importance of variables in explaining COVID-19 growth rate.
629 We fitted regression models starting from regions experiencing outbreaks up to February 27,
630 until we included all regions experiencing outbreaks up to May 31, 2020 (n = 586 regions). The
631 partial R^2 statistic (variance explained by each fixed effect) was taken as a measure of the
632 relative importance of variables. a) temperature calculated using the 30-days period; b)
633 temperature calculated using the $\Delta 14$ days period (see Supplement 1, Fig. S1 for details).

634
635 **Fig. 3.** Temporal variation of the relationships between independent variables and COVID-19
636 growth rate (standardized coefficients). We fitted regression models starting from regions
637 experiencing outbreaks up to February 27, until we included all regions experiencing outbreaks
638 up to May 31, 2020 (n = 586 regions). The plot includes temperature calculated using the 30-
639 days period; the pattern was identical if a $\Delta 14$ days period was used (see Supplement 1, Fig. S1
640 for details). Shaded areas represent 95% confidence bands. When confidence bands do not cross
641 the horizontal broken line (0 threshold), the effect of a given variable is statistically significant
642 ($P < 0.05$).

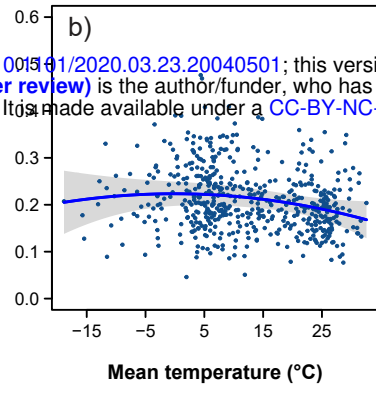
643
644 **Fig. 4.** Variation of COVID-19 growth rate in relation to local mean temperature (30-days
645 period), air pollution (PM 2.5) and stringency of containment measures. Partial regression plots
646 from mixed models of COVID-19 mean daily growth rates fitted for local outbreaks occurring up
647 to March 15 (n = 195 regions), April 15 (n = 529 regions) and May 15 (n = 577 regions) are
648 shown. The shaded areas are 95% confidence bands.

649
650

15 March dataset



15 April dataset



15 May dataset

